The Journal of Immunology

The Chemokine Receptors CXCR1 and CXCR2 Couple to Distinct G Protein-Coupled Receptor Kinases To Mediate and Regulate Leukocyte Functions

Sandeep K. Raghuwanshi, Yingjun Su, Vandana Singh, Katherine Haynes, Ann Richmond and Ricardo M. Richardson

J Immunol 2012; 189:2824-2832; Prepublished online 6 August 2012;
doi: 10.4049/jimmunol.1201114
http://www.jimmunol.org/content/189/6/2824

The Journal of Immunology is published twice each month by
The American Association of Immunologists, Inc.,
1451 Rockville Pike, Suite 650, Rockville, MD 20852

Print ISSN: 0022-1767 Online ISSN: 1550-6606.

The Chemokine Receptors CXCR1 and CXCR2 Couple to Distinct G Protein-Coupled Receptor Kinases To Mediate and Regulate Leukocyte Functions

Sandeep K. Raghuwanshi,* Yingjun Su,[†,‡] Vandana Singh,* Katherine Haynes,* Ann Richmond,[†,‡] and Ricardo M. Richardson*

The chemokine receptors, CXCR1 and CXCR2, couple to Gαi to induce leukocyte recruitment and activation at sites of inflammation. Upon activation by CXCL8, these receptors become phosphorylated, desensitized, and internalized. In this study, we investigated the role of different G protein-coupled receptor kinases (GRKs) in CXCR1- and CXCR2-mediated cellular functions. To that end, short hairpin RNA was used to inhibit GRK2, 3, 5, and 6 in RBL-2H3 cells stably expressing CXCR1 or CXCR2, and CXCL8-mediated receptor activation and regulation were assessed. Inhibition of GRK2 and GRK6 increased CXCR1 and CXCR2 resistance to phosphorylation, desensitization, and internalization, respectively, and enhanced CXCL8-induced phosphoinositide hydrolysis and exocytosis in vitro. GRK2 depletion diminished CXCR1-induced ERK1/2 phosphorylation but had no effect on CXCR2-induced ERK1/2 phosphorylation. GRK6 depletion had no significant effect on CXCR1 function. However, peritoneal neutrophils from mice deficient in GRK6 ($GRK6^{-/-}$) displayed an increase in CXCR2-mediated G protein activation but in vitro exhibited a decrease in chemotaxis, receptor desensitization, and internalization relative to wild-type ($GRK6^{+/+}$) cells. In contrast, neutrophil recruitment in vivo in $GRK6^{-/-}$ mice was increased in response to delivery of CXCL1 through the air pouch model. In a wound-closure assay, $GRK6^{-/-}$ mice showed enhanced myeloperoxidase activity, suggesting enhanced neutrophil recruitment, and faster wound closure compared with $GRK6^{+/+}$ animals. Taken together, the results indicate that CXCR1 and CXCR2 couple to distinct GRK isoforms to mediate and regulate inflammatory responses. CXCR1 predominantly couples to GRK2, whereas CXCR2 interacts with GRK6 to negatively regulate receptor sensitization and trafficking, thus affecting cell signaling and angiogenesis. ***The Journal of Immunology*****, 2012, 189: 2824–2832.**

CXCL8/IL-8 (IL-8) is a member of the CXC subfamily of chemokines that binds to seven transmembrane G protein-coupled receptors (GPCRs), CXCR1 and CXCR2, to mediate and regulate leukocyte accumulation and activation at sites of inflammation (1, 2). CXCR1 interacts predominantly with CXCL8, whereas CXCR2 also binds CXCL1, 2, 3, 5, and 7 (3). Upon activation, both receptors couple to pertussis toxin-sensitive Gαi proteins to activate phospholipase C, resulting in the generation of the intracellular messenger diacylglycerol and inositol 1,4,5-triphosphate. Following CXCL8 activation, CXCR1 and CXCR2 become desensitized and internalized (4, 5). In contrast, Gβγ subunits activate PI3K, leading to the phosphorylation of phosphoinositide (PI) (4,5) diphosphate to form PI (3,4,5) trisphosphate, which activates many signal-transduction pathways required for motility, growth, and gene expression.

*Department of Biology, Julius L. Chambers Biomedical/Biotechnology Research Institute, North Carolina Central University, Durham, NC 27707; [†]Department of Veterans Affairs, Nashville, TN 37212; and [‡]Department of Cancer Biology, Vanderbilt University School of Medicine, Nashville, TN 37232

Received for publication April 26, 2012. Accepted for publication July 6, 2012.

This work was supported by National Institutes of Health (NIH) Grants AI38910, CA156735, NIMHD P20 MD00175, and USAMRMC 07-1-0418 (to R.M.R.); NIH Grant CA34590 and the Department of Veterans Affairs (Senior Research Career Scientist) (to A.R.); and a Historically Black College and Universities Grant, Department of Veterans Affairs (to A.R. and R.M.R.).

Address correspondence and reprint requests to Dr. Ricardo M. Richardson, Julius L. Chambers Biomedical/Biotechnology Research Institute, North Carolina Central University, 1801 Fayetteville Street, Durham, NC 27707. E-mail address: mrrichardson@nccu.edu

Abbreviations used in this article: GPCR, G protein-coupled receptor; GRK, G protein-coupled receptor kinase; IL-8, CXCL8/IL-8; MPO, myeloperoxidase; PI, phosphoinositide; shRNA, short hairpin RNA.

Phosphorylation of GPCRs by GPCR kinases (GRKs) and recruitment of clathrin-binding adaptor proteins to the cell membrane are prerequisites for receptor desensitization (6, 7). Seven GRKs (GRK1–7) have been identified and characterized (8). GRK1 and GRK7 are exclusively expressed in the visual system: retinal rods and cones, respectively (9). GRK2, GRK3, GRK5, and GRK6 are expressed in most mammalian cell types, whereas GRK4 expression has been detected only in the testis, kidney, and cerebellum (9, 10). Genetic deletion in mouse and suppression of expression of specific GRKs in transfected cell lines by small interfering RNA targeting indicated that GPCRs may couple to specific GRKs to modulate distinct, as well as similar, cellular responses (11–14).

The role of GRK isoforms in chemokine receptor functions remains ill-defined. Decreased expression of GRK2 correlates with increased cellular responses to the CC receptors CCR2 and CCR5 (15–17). CCR7 was shown to couple to both GRK3 and GRK6 to undergo receptor phosphorylation and desensitization, but only GRK6 phosphorylation led to MAPK activation (18). Neutrophils deficient in GRK6 displayed increased CXCR4 activation and resistance to desensitization (19). Busillo et al. (20) also showed that GRK2 and GRK3 are critical for CXCR4 desensitization and postendocytic signaling. Altogether, these data suggest that the chemokine receptors couple to specific GRKs to mediate and regulate cellular functions.

Previous studies from our laboratory (4, 5) and those of other investigators (21–23) showed that GRK-mediated phosphorylation of specific amino acid residues in the cytoplasmic tails of CXCR1 and CXCR2 is critical for β-arrestin association, receptor internalization, and receptor-induced postendocytic signals in some cell types. In this study, we sought to determine the role of dif-

www.jimmunol.org/cgi/doi/10.4049/jimmunol.1201114

ferent GRKs in CXCR1- and CXCR2-mediated cellular functions. To that end, RBL-2H3 cell lines, in which the expression of GRK2, 3, 5, or 6 was suppressed by short hairpin RNA (shRNA), and mouse models of inflammation deficient in GRK6 were generated to assess receptor activation and regulation. Taken together, the results indicate that, upon activation by CXCL8, CXCR1 and CXCR2 interact with distinct GRK isoforms to modulate leukocyte functions.

Materials and Methods

Materials

[^{32}P]Orthophosphate (8500–9120 Ci/mmol), myo-[2-^{3}H]inositol (24.4 Ci/mmol), and [^{125}I]CXCL8 were purchased from Perkin Elmer. IL-8 (CXCL8) and CXCL1 were obtained from PeproTech (Rocky Hill, NJ). Indo-1, AM, Geneticin (G418), and all tissue culture reagents were purchased from Invitrogen (Gaithersburg, MD). Monoclonal 12CA5 Ab, protein G-agarose, and protease inhibitors were purchased from Roche (Indianapolis, IN). Anti-human IL-8RA (CXCR1) and IL-8RB (CXCR2) Abs were purchased from BD Pharmingen (San Jose, CA). Anti-GRK2/3 and anti-GRK5/6 were obtained from Millipore (Billerica, MA). Rabbit anti-ERK1/2 and anti–phospho-ERK1/2 Abs were purchased from Cell Signaling (Beverly, MA). Mission shRNA Plasmid DNA (pLKO.1-puro) for GRK subtypes were purchased from Sigma Life Sciences (St. Louis, MO) or obtained from Dr. Hydar Ali (University of Pennsylvania, Philadelphia, PA). All other reagents were from commercial sources.

Cell culture and transfection

RBL-2H3 cells were maintained as monolayer cultures in DMEM supplemented with 15% heat-inactivated FBS, 2 mM glutamine, penicillin (100 U/ml), and streptomycin (100 mg/ml) (24). RBL-2H3 cells (1×10^7) were transfected by electroporation with 20 μg pcDNA3 containing the receptor cDNAs, and Geneticin-resistant cells were cloned into single cells and confirmed by FACS analysis. The levels of protein expression were monitored by FACS analysis (25). For shRNA-mediated gene silencing, RBL-2H3 cells (1×10^7 cells) were transfected by electroporation with 20 μg Mission pLKO.1-puro containing shRNA for GRK2, GRK3, GRK5, GRK6, or control plasmid. A mixed population of puromycin-resistant cells was cloned into single cell using the limiting-dilution method. Levels of mRNA transcript and protein expression were monitored by real-time PCR and Western blotting.

FACS analysis

For flow cytometric analysis, RBL cells were detached by Versene treatment, washed with HEPES-buffered HBSS, and resuspended in the same medium. Cells (1–5 $\times 10^6$ cells) were incubated with anti-CXCR1 or anti-CXCR2 Abs (1 μg/ml) in a total volume of 400 μl HEPES-buffered HBSS for 60 min at 4°C. The cells were then washed and incubated with FITC–anti-mouse IgG for 60 min at 4°C. Cells were then washed and analyzed for cell surface expression of the receptor on a Beckton Dickenson FACScan cytometer (5).

Radioligand binding assays and receptor internalization

For receptor internalization, RBL-2H3 cells were subcultured overnight in 24-well plates (0.5×10^6 cells/well) in growth medium. Cells were then rinsed with DMEM supplemented with 20 mM HEPES (pH 7.4) and 10 mg/ml BSA and incubated with ligand for 0–60 min at 37°C. Then, cells were washed with ice-cold PBS and [^{125}I]CXCL8 binding (0.1 nM) was carried out, as described previously (5). Nonspecific radioactivity bound to cells was determined in the presence of 500 nM unlabeled CXCL8 (26).

PI hydrolysis, β-hexosaminidase release, and calcium measurement

RBL-2H3 cells were subcultured overnight in 96-well culture plates (50,000 cells/well) in inositol-free medium supplemented with 10% dialyzed FBS and 1 μCi/ml [^{3}H]inositol. The generation of inositol phosphates was determined, as reported (24, 27). For calcium mobilization, cells (5×10^6) were washed with HEPES-buffered saline and loaded with 1 μM Indo-1, AM in the presence of 1 μM pluronic acid for 30 min at room temperature. The cells were then washed with HEPES and resuspended in 1.5 ml Sirganian buffer. Intracellular calcium increase in the presence or absence of ligands was measured, as described previously (28).

Receptor phosphorylation

Receptor phosphorylation was performed, as described previously (5, 25). RBL-2H3 cells (5×10^6) expressing the receptors were incubated with [^{32}P]orthophosphate (150 μCi/dish) for 90 min. Then, labeled cells were stimulated with the indicated ligands for 5 min at 37°C. Cells were then washed with ice-cold PBS and solubilized in 1 ml radioimmunoprecipitation assay buffer containing 50 mM Tris-HCl (pH 7.5), 150 mM NaCl, 1% Nonidet P-40, 0.5% sodium deoxycholate, and 0.1% SDS. Cell lysates were immunoprecipitated with specific Abs against the N terminus of CXCR1 or CXCR2, analyzed by SDS electrophoresis, and visualized by autoradiography.

Measurement of ERK activity

For ERK activity, RBL-2H3 cells (3×10^6) expressing CXCR1 or CXCR2 or peritoneal neutrophils from GRK6$^{-/-}$ mice and control littermates (GRK6$^{+/+}$) were washed three times with PBS and then resuspended in PBS containing CXCL8 (100 nM) for different periods of time at 37°C. The reactions were stopped with ice-cold PBS; cells were collected by centrifugation, lysed with radioimmunoprecipitation assay, and assayed for protein concentration, as described previously (29). Equal amounts of protein (20 μg) from each sample were resolved by 10% SDS-PAGE, transferred to a nitrocellulose membrane, and probed with Ab against either ERK1/2 or phospho-ERK1/2. Detection was carried out with HRP-conjugated sheep anti-mouse Ab and by ECL.

Animals

All experiments were approved by and conformed to the guidelines of the Animal Care Committee of North Carolina Central University, Vanderbilt University School of Medicine, and/or Meharry Medical College. Animals were housed five per cage in a room at 22 ± 5°C, with an alternating 12-h light–dark cycle. GRK6-deficient mice (C57/BL6 background) were kindly provided by Dr. Robert J. Lefkowitz (Howard Hughes Medical Institute, Duke University Medical Center, Durham, NC). Male and female mice were evaluated; age- and sex-matched littermates were used as controls. All of the mice were genotyped at the age of 3 wk; DNA samples were prepared from the tail tips with a DNeasy tissue kit (QIAGEN USA) and subjected to triplex PCR, as described (30, 31).

Peritoneal recruitment of neutrophils

Zymosan was prepared in PBS to a final concentration of 1 mg/ml, and 1.0 ml was injected into the peritoneum of control and GRK6-deficient mice. Mice were euthanized by CO_2 asphyxiation, and the peritoneal cavity was lavaged at 4 h postinjection with 8 ml ice-cold RPMI 1640 containing 2% FBS and 2 mM EDTA. Cells were collected by centrifugation, counted, and stained with Diff-Quick to assess the percentage of neutrophils (32).

Plasma membrane preparations

Zymosan-elicited peritoneal neutrophils were resuspended in homogenizing buffer containing 25 mM Tris Buffer (pH 7.6), 5 mM $MgCl_2$, and protease inhibitors (1 μl/ml) and homogenized for 30 s with a Polytron. The homogenate was centrifuged at 150 × *g* for 5 min, and the supernatant was collected. The procedure was repeated twice, and the pooled supernatant was centrifuged at 10,000 × *g* for 10 min. The pellet was resuspended in the same buffer (1 mg of protein/ml) and stored at −80°C until use.

Intracellular Ca^{2+} mobilization, receptor internalization, GTPase activity, and chemotaxis

Zymosan-elicited peritoneal neutrophils (3×10^6 cells) were washed with HEPES-buffered saline and loaded with 1 μM Indo-1, AM for 30 min at room temperature. The cells were washed and resuspended in 1.5 ml HEPES-buffered saline, and intracellular Ca^{2+} mobilization was measured as described (32). For receptor internalization, 5×10^5 neutrophils were resuspended in 250 μl HBSS containing 25 mM HEPES and 0.1% BSA. Cells were treated with recombinant murine CXCL1 (100 nM) at 37°C for different time periods. Reactions were stopped by adding 1 ml ice-cold HBSS, followed by centrifugation at 1000 rpm for 2 min. Then, cells were washed three times and assayed for [^{125}I]CXCL1 binding, as previously described (32). For GTPase activity, membranes (10 μg membrane preparations/assay) were assayed, as described (32, 33), in the presence or absence of 1 μM recombinant murine CXCL1. For chemotaxis, neutrophils (~50,000) were incubated at 37°C with different concentrations of ligands. Chemotaxis was assessed in 48-well microchemotaxis chambers using polyvinylpyrrolidone-free membranes with 8-μm pores, as described previously (29). The results are representative of three separate experiments.

Murine skin air pouch model of inflammation

GRK6$^{-/-}$ and littermate control mice (6–8 wk) were anesthetized with isoflurane, and dorsal air pouches were raised by injecting 3 ml sterile air s.c. on days 0 and 3, as described previously (34–36). On day 6, the mice were anesthetized with isoflurane, and inflammation in the air pouch was induced by local injection of recombinant murine CXCL1 (100 pmol) dissolved in 0.5 ml sterile PBS. Mice were sacrificed 4 h after CXCL1 injection by CO_2 asphyxiation, and air pouches were lavaged three times with 3 ml PBS. Cells were collected by centrifugation at 2000 rpm for 5 min at room temperature. The supernatants were removed, and the cells were resuspended in 10 ml PBS and counted. Aliquots of the cell suspension were stained with Wright–Giemsa and enumerated by light microscopy (~90% of the exudates are neutrophils).

Mouse skin excisional wounding procedures

Excisional punch wounds were made, as described previously, with slight modifications (32, 37). GRK6$^{-/-}$ and wild-type mice (6–8 wk old) were anesthetized with an i.p. injection of ketamine (100 mg/kg body weight) and xylazine (10 mg/kg body weight) (Fort Dodge Animal Health, Fort Dodge, IA). The dorsal surface of the mouse was cleaned, shaved, and sterilized with betadine solution (Purdue Frederick, Norwalk, CT) and 70% ethanol. Two full-thickness excisional wounds were made in the dorsal paravertebral region with a 4-mm-diameter punch (Acu-Punch, Fort Lauderdale, FL). Wounds were covered and kept under occlusion by Spray Bandage (Curad; Beiersdorf, Wilton, CT). Analgesics (Buprenex; Reckitt & Colman Pharmaceuticals, Richmond, VA) were administered i.p. at a dosage of 4.5 μg/kg body weight. All wounds were monitored visually daily for signs of infection.

Myeloperoxidase assay

Myeloperoxidase (MPO) activity was assayed, as described previously (37, 38). Briefly, wound tissues from postwounding days 1–3 were harvested, snap-frozen in liquid nitrogen, and homogenized in 1 ml phosphate buffer containing 0.5% hexadecyl trimethyl ammonium bromide in 50 mM phosphate buffer (pH 6). Hexadecyl trimethyl ammonium bromide is a detergent that releases MOP from primary granules of neutrophils. After sonication on ice for 15 s (Sonic Model 300; Fisher Scientific), tissue homogenates were centrifuged at 20,000 × *g* for 20 min at 4°C. The supernatants were collected, and their protein concentrations were measured using the Bio-Rad protein determination assay. Aliquots of the supernatant containing equivalent amounts of 50 μg protein were mixed with 500 μl potassium phosphate buffer (50 mM [pH 6.0]) containing 0.2% *O*-Dianisidine hydrochloride (Sigma Chemical, St. Louis, MO) and 0.0005% H_2O_2. The reaction was initiated by the addition of H_2O_2. The change in absorbance at 490 nm during a 2-min reaction period was measured spectrophotometrically, using the Beckman-DU 7000 (Beckman Coulter, Fullerton, CA). The absorbance values were compared for each aliquot of wound tissue lysate from wild-type and GRK6$^{-/-}$ mice. The MPO values of nonwounded skin tissues from each genotype served as controls.

Wound-closure analysis

Wounds were collected on postwounding days 3, 5, 7, and 10. Each wound was centrally bisected, embedded in paraffin, and sectioned at 6 μm, followed by staining with Gomori's Trichrome. For wild-type or GRK6$^{-/-}$ mice, eight wound tissues from four mice were excised and analyzed for each time point. The percentage of wound resurfacing was assessed by morphometric analysis (39, 40) on tissue slide images using Image-Pro Plus software.

Statistical analyses

Results are expressed as mean ± SEM. Statistical differences between groups were determined by the Student two-tailed paired *t* test; p values < 0.05 were considered statistically significant.

Results

Role of GRKs in CXCR1 and CXCR2 desensitization

To determine the role of GRKs in CXCR2 regulation, RBL-2H3 cells stably expressing CXCR2 were transiently transfected with Mission pLKO.1-puro containing shRNA for GRK2, GRK3, GRK5, GRK6, or control plasmid. Forty-eight hours post-transfection, cells were analyzed by RT-PCR (data not shown) and immunoblotting. As shown in Fig. 1A, expression of GRK2,

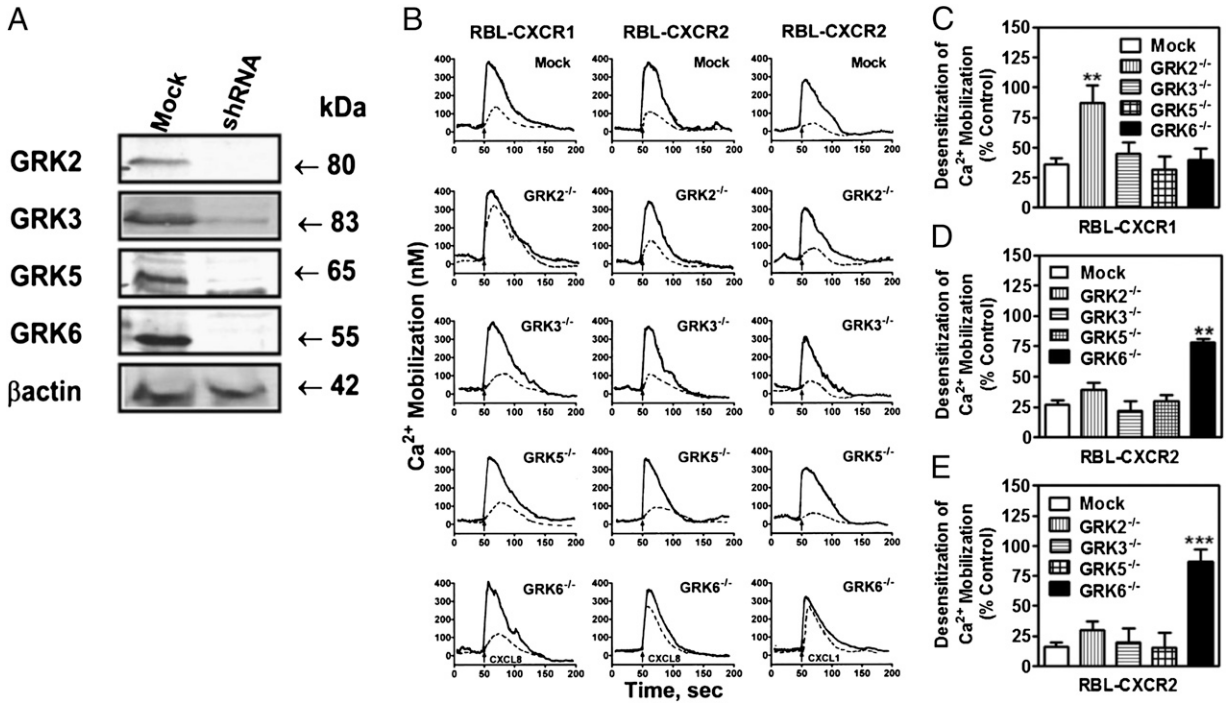

FIGURE 1. Transient inhibition of GRK2, GRK3, GRK5, and GRK6 expression in RBL-2H3 cells and their effects on CXCR1 and CXCR2 desensitization. (**A**) RBL cells (5×10^5 cells/well) were transfected with 20 μg of control (mock) or small interfering RNA specific for GRK2, GRK3, GRK5, or GRK6. Forty-eight hours posttransfection, cells were lysed and analyzed by immunoblotting. (**B**) For receptor desensitization, GRK-deficient and control (mock-transfected) RBL cells (5×10^6 cells) expressing CXCR1 or CXCR2 were loaded with Indo-1, AM in the presence or absence of 10 nM CXCL8 (*left* and *middle columns*) or CXCL1 (*right column*) for 30 min and assayed for CXCL8- or CXCL1-induced (10 nM) intracellular Ca^{2+} mobilization. Traces shown are representative of three to five experiments. (**C**–**E**) Desensitization was determined as the percentage of control, which is the peak of intracellular Ca^{2+} mobilization obtained in the absence of pretreatment. Data are the average of at least three traces. $^{**}p < 0.01$, $^{***}p < 0.001$, Student *t* test.

GRK3, GRK5, and GRK6 was inhibited by 90–95% relative to control cells. For receptor desensitization, the peak of CXCL8-induced intracellular Ca^{2+} mobilization was measured in cells pretreated with 10 nM CXCL8 and compared with that of untreated cells. Pretreatment of RBL-CXCR1 cells (Fig. 1B, *left column*, mock) or RBL-CXCR2 cells (Fig. 1B, *middle column*, mock) desensitized response to a second dose by ~63% (Fig. 1C, mock) and ~75% (Fig. 1D, mock), respectively. Loss of GRK2 expression ($GRK2^{-/-}$), but not loss of GRK3 ($GRK3^{-/-}$), GRK5 ($GRK5^{-/-}$), or GRK6 ($GRK6^{-/-}$) expression, significantly increased CXCR1 resistance to desensitization (~10% versus ~63% desensitization for $GRK2^{-/-}$ and mock cells, respectively), relative to control cells (Fig. 1B, 1C). In contrast, $GRK6^{-/-}$ cells (but not $GRK2^{-/-}$, $GRK3^{-/-}$, or $GRK5^{-/-}$ cells) exhibited a significant increase in CXCR2 resistance to desensitization (~25% versus ~75% desensitization for $GRK6^{-/-}$ and mock cells, respectively, Fig. 1B, 1D).

In addition to CXCL8, CXCR2 interacts with CXCL1, 2, 3, 5, 6, and 7 to mediate cellular responses (41). To further assess the specificity of the CXCR2/GRK6 interaction, we measured CXCL1-induced receptor desensitization in RBL-CXCR2 cells deficient in GRKs (Fig. 1B, *right column*). As shown in Fig. 1E, only $GRK6^{-/-}$ cells displayed a significant increase in receptor resistance to desensitization (~15% versus ~91% desensitization for $GRK6^{-/-}$ and control mock cells, respectively). These results mirrored the ones obtained with CXCL8 and indicated that the effect of GRK6 deficiency likely is receptor specific.

Effect of GRK2 and GRK6 inhibition on CXCL8-induced receptor activation and regulation

To further assess the specificity of GRKs in receptor activation and regulation, puromycin-resistant RBL-CXCR1 (Fig. 2A) and RBL-CXCR2 (Fig. 2B) cells, in which GRK2 (CXCR1-$GRK2^{-/-}$ and CXCR2-$GRK2^{-/-}$) and GRK6 (CXCR1-$GRK6^{-/-}$ and CXCR2-$GRK6^{-/-}$) expression was stably suppressed, were generated by single-cell cloning and confirmed by real-time PCR (data not shown) and immunoblotting (Fig. 2C). The dose response of CXCL8-induced β-hexosaminidase release was measured to assess receptor activation. Maximum responses were ~35 and ~23% of total for CXCR1-$GRK6^{+/+}$ (Fig. 3A) and CXCR2-$GRK6^{+/+}$ (Fig. 3B) cells, respectively. GRK6 inhibition had no effect on CXCR1-mediated exocytosis (Fig. 3A), but it caused a ~40% increase in response to CXCR2 (Fig. 3B). Absence of GRK6 decreased CXCR2 phosphorylation (Fig. 3D, *right panel*, *lane 8* versus *lane 6*) and internalization (Fig. 3C), with no effect on CXCR1 (Fig. 3C, 3D, *left panel*).

The dose response of CXCL8-induced PI hydrolysis and β-hexosaminidase release was also measured in GRK2-deficient cells. As shown in Fig. 4, CXCR1-$GRK2^{-/-}$ cells exhibited a marked increase in PI hydrolysis (~35%) (Fig. 4A) and β-hexosaminidase release (~40%) (Fig. 4C) relative to control CXCR1-$GRK2^{+/+}$ cells. GRK2 inhibition had no effect on CXCR2-mediated responses (Fig. 4B, 4D).

Attenuation of GRK2 also increased CXCR1 resistance to phosphorylation (Fig. 4F, *left panel*, *lane 4* versus *lane 2*) and internalization (Fig. 4E), but it had no effect on CXCR2 (Fig. 4E, 4F, *right panel*, *lanes 8* versus *lane 6*) relative to control $GRK2^{+/+}$ cells.

Effect of GRK2 and GRK6 on CXCL8-induced ERK1/2 activation

To determine the effect of GRK2 and GRK6 in MAPK activation, RBL-CXCR1 and RBL-CXCR2 cells were stimulated with CXCL8 (100 nM) for different periods of time, and cells lysates were assayed for ERK1/2 phosphorylation. As previously shown (25, 33), CXCR1 and CXCR2 induced time-dependent ERK1/2 phosphorylation (Fig. 5). GRK2 depletion ($GRK2^{-/-}$) significantly inhibited CXCR1-mediated ERK1/2 phosphorylation (Fig. 5A, 5C), with no significant effect on CXCR2 (Fig. 5B, 5D). GRK6 knockdown had no significant effect on CXCR1- or CXCR2-mediated ERK1/2 phosphorylation (Fig. 5).

Effect of GRK6 deletion on leukocyte functions

To further determine the effect of GRK6 inhibition on CXCR2 functions, zymosan-induced peritonitis was used to recruit neutrophils into the peritoneal cavity of GRK6-deficient mice ($GRK6^{-/-}$) and littermates ($GRK6^{+/+}$). Membranes were prepared and assayed for murine CXCL1-induced G protein activation. Membrane preparations from $GRK6^{-/-}$ peritoneal neutrophils displayed a robust increase (~40%) in CXCL1-mediated response (~1.3 pmol ^{32}Pi released/mg protein) relative to $GRK6^{+/+}$ cells (~0.7 pmol ^{32}Pi released/mg protein) (Fig. 6A).

CXCL1-induced intracellular Ca^{2+} mobilization in peritoneal neutrophils was also measured to assess receptor desensitization. As shown in Fig. 6B, pretreated neutrophils from $GRK6^{+/+}$ animals showed ~70% decrease in CXCL1-mediated Ca^{2+} mobilization relative to untreated cells (225 ± 25 and 69 ± 27 nM for control and pretreated cells, respectively). Cells from $GRK6^{-/-}$ animals displayed only ~20% desensitization (244 ± 41 and 197 ± 59 nM for control and pretreated cells, respectively), which did not reach statistical significance. These results mirrored the one obtained with CXCR2-$GRK6^{-/-}$ RBL cells and indicated that deletion of GRK6 increased CXCR2 resistance to desensitization.

Receptor internalization was also assessed in cells pretreated with CXCL1 (100 nM) for different periods of time (Fig. 6C). $GRK6^{+/+}$ cells showed a rapid decrease in receptor binding (~95% after 30 min of pretreatment). However, CXCR2 from $GRK6^{-/-}$ cells was more resistant to internalization (~75% after 30 min of

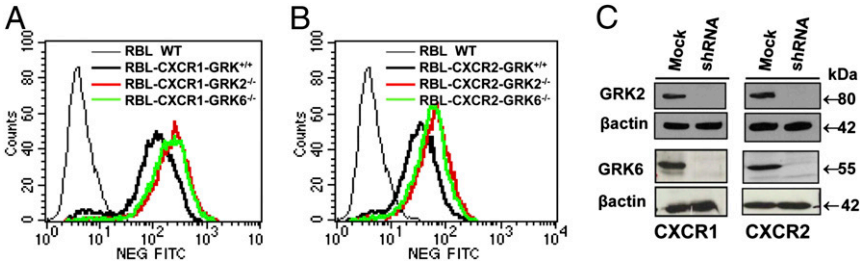

FIGURE 2. Stable knockdown of GRK2 and GRK6 expression in RBL-2H3 cells stably expressing CXCR1 and CXCR2. Representative graph of FACS analysis showing surface expression of CXCR1 (**A**) and CXCR2 (**B**) in RBL-2H3 cells after staining with CXCR1- or CXCR2-specific Abs. (**C**) RBL-2H3 cells expressing CXCR1 (*left panel*) or CXCR2 (*right panel*) were transfected with scrambled shRNA control lentivirus (mock) or shRNA lentivirus specific for GRK2 or GRK6 knockdown. Puromycin-resistant cells were selected, and single clones were generated and analyzed by immunoblotting.

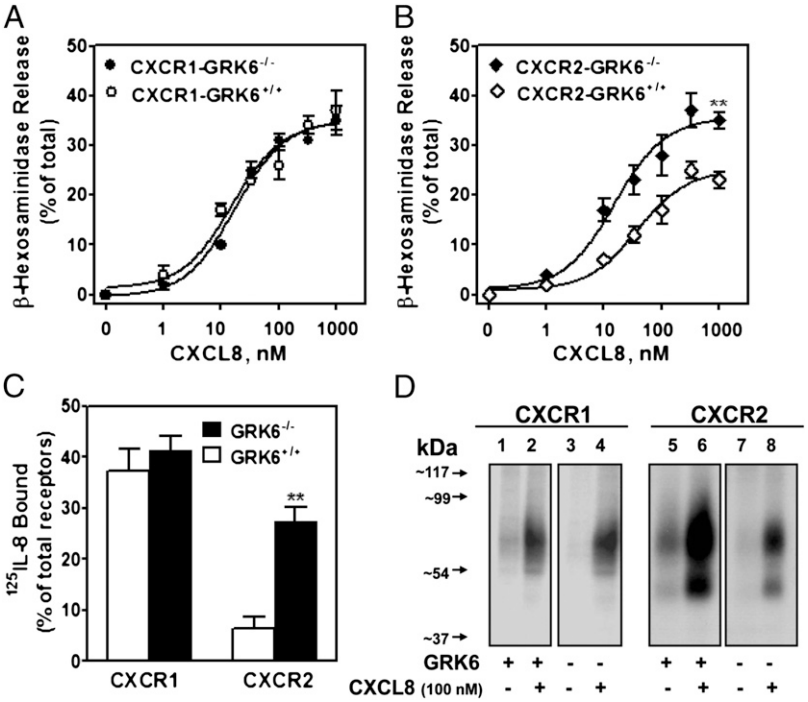

FIGURE 3. GRK6 inhibition enhances CXCR2-mediated exocytosis and decreases receptor phosphorylation and internalization. (**A** and **B**) For β-hexosaminidase release, cells (50,000/well) were cultured overnight, washed with HEPES-buffered saline, and stimulated with different concentrations of CXCL8 for 10 min. Supernatant (15 μl) was removed, and β-hexosaminidase release was measured. Data represent the percentage of total β-hexosaminidase release from cell lysates. The experiments were repeated four times with similar results. (**C**) For receptor internalization, cells (0.5×10^6/well) were treated with CXCL8 (100 nM) or vehicle control for 60 min and assayed for [^{125}I]CXCL8 binding. Data represent the percentage of total [^{125}I]CXCL8 bound to control (untreated) cells. (**D**) For receptor phosphorylation, ^{32}P-labeled GRK6$^{+/+}$ (*lanes 1, 2*) and GRK6$^{-/-}$ (*lanes 3, 4*) RBL cells (5×10^6 cells/60-mm plate) expressing CXCR1 (*left panels*) or CXCR2 (*right panels*) were incubated for 5 min with (*lanes 2, 4*) or without (*lanes 1, 3*) 100 nM CXCL8. Cells were lysed, immunoprecipitated with CXCR1 and CXCR2 Abs, analyzed by SDS-PAGE, and autoradiographed. The results shown are from a representative experiment that was repeated twice. $^{**}p < 0.01$.

pretreatment). CXCL1-mediated chemotaxis in vitro was significantly inhibited in peritoneal neutrophils from GRK6$^{-/-}$ animals relative to control GRK6$^{+/+}$ cells (Fig. 6D).

We next determined the effect of GRK6 inhibition on CXCR2-mediated MAPK activation by measuring CXCL1-induced ERK1/2 phosphorylation (Fig. 7A). GRK6$^{+/+}$ neutrophils showed a rapid (~23% at 1 min), but transient, increase in CXCL1-induced ERK1/2 phosphorylation (Fig. 7B, ○). However, the response in GRK6$^{-/-}$ cells was delayed (~10% at 1 min) but sustained (Fig. 7B, ●). However, the transient effect observed at ~1 min in GRK6$^{-/-}$ cells was not statistically significant ($p > 0.05$) relative to control (GRK6$^{+/+}$ cells).

Role of GRK6 in CXCR2-mediated neutrophil migration in vivo

Deletion of β-arrestin-2 inhibited CXCL1-mediated chemotaxis in vitro but enhanced neutrophil infiltration in vivo in the air pouch model of skin inflammation (32). To determine whether GRK6 deletion affected neutrophil migration in vivo, air pouches were created in GRK6$^{-/-}$ mice and their littermates (GRK6$^{+/+}$). PBS-induced neutrophil recruitment in GRK6$^{+/+}$ mice (~1.6×10^6 cells) was similar to that of GRK6$^{-/-}$ animals (~1.8×10^6 cells) (Fig. 8A, white bars). In contrast, injection of CXCL1 (100 pmol) into the air pouch 6 d after it was raised induced greater neutrophil accumulation (~ 5.7×10^6 cells) in GRK6$^{-/-}$ mice relative to control GRK6$^{+/+}$ animals (~3.1×10^6 cells; $p < 0.05$) (Fig. 8A, black bars).

Neutrophil infiltration was further determined by MPO assays performed on excisional wound tissue extracts. MPO activity of wild-type and GRK6$^{-/-}$ mouse wounds increased sharply at 24 h postwounding and was sustained over postwound day 3 (Fig. 8B). However, the MPO activity in wounds from GRK6$^{-/-}$ mice was significantly higher (~1 and ~2-fold increase postwounding day 1 and 2, respectively) than was that in wounds from wild-type mice (Fig. 8B). This was followed by a marked decrease in MPO activity to the level exhibited in wounds from wild-type mice at postwounding day 3.

Wound re-epithelialization was also increased in GRK6$^{-/-}$ mice relative to wild-type animals. The percentage of epidermal resurfacing for GRK6$^{+/+}$ mouse wounds at days 3, 5, and 7 was 37, 68, and 97%, respectively. Wound resurfacing percentages for GRK6$^{-/-}$ mice were increased significantly to 58% at day 3 ($p < 0.05$). Wounds from both genotypes were similar at days 5 and 7, and each was completely re-epithelialized by postwounding day 10 (Fig. 8C).

Discussion

CXCR1 and CXCR2 bind the proangiogenic ELR-positive (glutamic acid-leucine-arginine) chemokines to mediate cellular responses, including chemotaxis and angiogenesis. These responses are regulated by phosphorylation of the receptors at specific serine and threonine residues of the C terminus, leading to uncoupling of the receptor from G protein and, thereby, promoting receptor desensitization and downregulation (11). CXCR1 and CXCR2 are phosphorylated via two mechanisms: a protein kinase C-dependent mechanism and a GRK-dependent mechanism (4, 28, 42). GRKs are known to phosphorylate the agonist-occupied receptor to promote arrestin recruitment and receptor internalization (10). Upon CXCL8 activation, CXCR1 internalizes slowly (~45% after 60 min) but recovers rapidly (~100% after 90 min), whereas CXCR2 internalizes rapidly (~95% after 5–10 min) but recovers slowly (~35% after 90 min) at the cell surface (4, 5, 42–45). This distinction appears to play a critical role in the ability of the receptors to activate certain leukocyte responses, including respiratory burst and cross-regulatory and postendocytic signals (4, 5). Thus, defining the role of specific GRK isoforms in CXCR1 and CXCR2 activation and regulation is essential to the understanding of the distinct roles played by these receptors in inflammation. The results identified GRK2 and GRK6 as critical kinases in the regulation of CXCL8-mediated cellular functions. First, suppression of GRK2 and GRK6 expression significantly increased CXCR1 and CXCR2 resistance, respectively, to CXCL8-mediated receptor phosphorylation, desensitization ($p < 0.01$), and internalization ($p < 0.05$) (Figs. 1, 3, 4). Second, as a consequence of GRK2 or GRK6 inhibition, both receptors displayed increased CXCL8-induced cellular responses, including PI hydrolysis and β-hexosaminidase release, but decreased ERK1/2

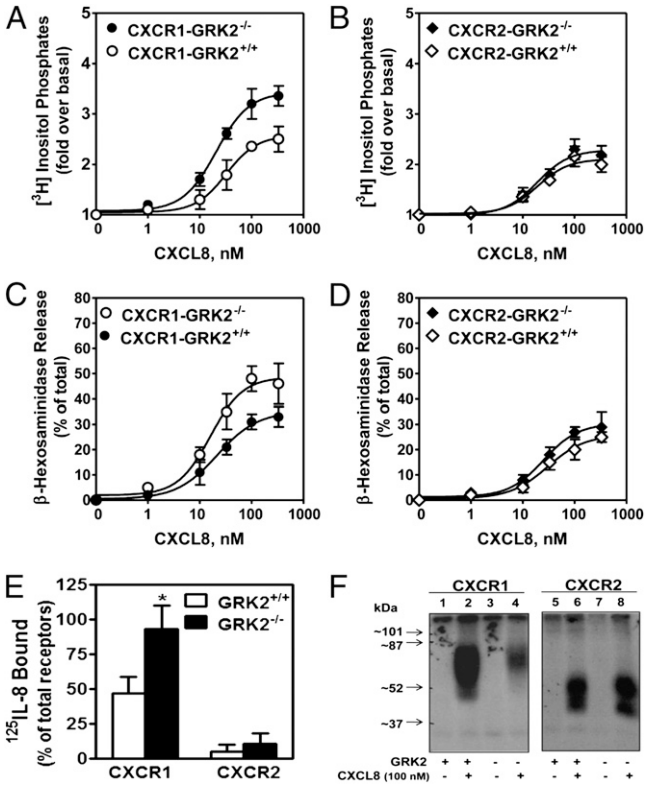

FIGURE 4. GRK2 knockdown increases CXCR1-mediated exocytosis but decreases receptor phosphorylation and internalization. (**A** and **B**) For the generation of inositol phosphates, cells (50,000/well) were cultured overnight in the presence of [^{3}H]inositol (1 μC/ml), washed with HEPES-buffered saline, preincubated for 10 min at 37°C with HEPES-buffered saline containing 10 mM LiCl in a total volume of 200 μl, and stimulated with different concentrations of CXCL8 for 10 min. The supernatant was used to determine the release of inositol phosphates. (**C** and **D**) β-hexosaminidase release was measured as described for (A) and (B). Data represent the fold change over basal PI (A, B) or the percentage of total β-hexosaminidase release from cell lysates (C, D) and are the average of three experiments performed in triplicate. Receptor internalization (**E**) and phosphorylation (**F**) were measured as described in the legend of Fig. 3. The results are the mean (E) or a representative (F) of three experiments. *$p < 0.05$, Student t test.

activation (Figs. 3–5). Third, consistent with the results obtained in RBL cells, peritoneal neutrophils from mice deficient in GRK6 expression exhibited a significant increase in murine CXCR2-mediated G protein activation and receptor resistance to desensitization and internalization but a decrease in chemotaxis relative to cells from wild-type GRK6$^{+/+}$ mice (Fig. 6).

In contrast to the decrease in chemotaxis observed in vitro, CXCL1-induced neutrophil accumulation into the dorsal air pouch generated in GRK6$^{-/-}$ mice showed a 2-fold increase relative to control GRK6$^{+/+}$ animals (Fig. 8A). Peritoneal neutrophils from mice deficient in β-arrestin-2 expression (βarr2$^{-/-}$) also displayed decreased chemotaxis in vitro but increased recruitment in the air pouch model of inflammation (32). In both cases, the knockout cells showed increased CXCR2-mediated G protein activation in membranes and receptor resistance to desensitization and internalization. Previous studies with transfected cell lines expressing phosphorylation-deficient mutants of CXCR1 and CXCR2 showed that decreased receptor internalization correlated with decreased CXCL8-mediated chemotaxis but increased receptor-mediated G protein activation, second messenger production, and exocytosis (5). Thus, the increase in CXCL1-induced neutrophil accumulation into the air pouch relative to wild-type animals could be a consequence of the increased receptor activity that resulted in greater secretion of proteases and tissue permeability, thereby facilitating cell migration. A second explanation could be the difference between the air pouch and the Transwell assays used to measure chemotaxis. A third explanation could be that β-arrestin plays a negative-regulatory role, such that loss of this negative regulator results in enhanced chemotaxis that is more apparent in vivo than in vitro, possibly involving the microenvironment of the cells. Interestingly, as was the case with βarr2$^{-/-}$ mice (32), cutaneous excisional wounds in GRK6$^{-/-}$ animals displayed a significant increase in MPO activity in the wound bed, as well as rapid wound re-epithelialization relative to GRK6$^{+/+}$ animals (Fig. 8B, 8C), which likely indicates greater CXCR2-induced angiogenesis.

It was shown recently that inhibition of GRK6 in mast cells promoted ERK1/2 phosphorylation but attenuated C3aR-mediated degranulation (46). However, inhibition of GRK6 in the RBL-2H3 mast cell line had no significant effect on CXCR2-mediated ERK1/2 phosphorylation, but it enhanced β-hexosaminidase release in response to CXCL8 (Figs. 3, 5). This difference likely indicates that the two receptors couple to distinct pathways to activate MAPK and mediate granule release in mast cells. Suppression of β-arrestin-1 expression in mast cells inhibited C3aR-mediated ERK1/2 activation (47). In contrast, inhibition of β-arrestin-2, not β-arrestin-1, was shown to decrease CXCR2-induced ERK1/2 activation (48). In addition, attenuation of GRK6 had no effect on C3aR desensitization, but it increased CXCR2

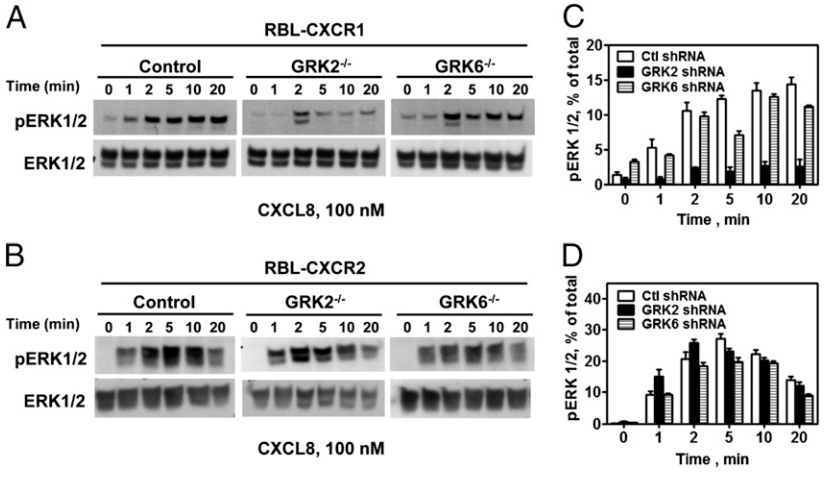

FIGURE 5. Effect of GRK2 and GRK6 knockdown on CXCR1-induced (**A**) or CXCR2-induced (**B**) ERK1/2 phosphorylation: RBL-2H3 cells were stimulated with CXCL8 (100 nM) for 0–20 min. ERK1/2 phosphorylation and total ERK were determined by Western blotting using anti–phospho-ERK1/2 (pERK1/2) and anti-total ERK1/2 (ERK1/2) Abs, respectively. Results shown are the percentage of total ERK and are the average of three experiments (**C**) for CXCR1 and (**D**) for CXCR2.

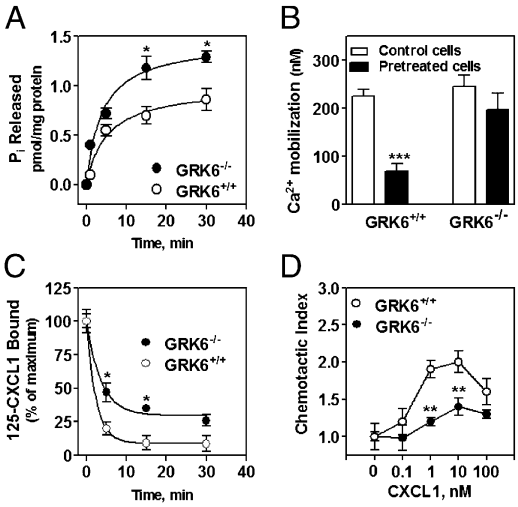

FIGURE 6. CXCL1-induced GTPase activity (**A**), intracellular Ca^{2+} mobilization (**B**), chemotaxis (**D**), and receptor internalization (**C**) in neutrophils from mice deficient in GRK6 ($GRK6^{-/-}$) relative to wild-type mice ($GRK6^{+/+}$). Zymosan-elicited peritoneal neutrophils were collected from mice deficient in GRK6 ($GRK6^{-/-}$) and control littermates ($GRK6^{+/+}$). (A) Membranes were prepared from zymosan-elicited peritoneal neutrophils and assayed for time-dependent CXCL1-stimulated ^{32}Pi released. Results shown are representative of one of two experiments performed in triplicate. (B) Cells (3×10^6 cells) were Indo-1, AM loaded, pretreated or not with CXCL1 (100 nM), and stimulated with 10 nM CXCL1. The data shown are representative of at least three traces. (C) Cells (0.5×10^6 cells) were treated with CXCL1 (100 nM) for different periods of time and assayed for [^{125}I]CXCL1 binding. Data represent the percentage of total [^{125}I]CXCL8 bound to control (untreated) cells. (D) Cells were incubated with calcein AM ionophore for 30 min and resuspended (1.0×10^5/20 ml) in RPMI 1640 without phenol red. Different concentrations of CXCL8 were loaded in a Neuro Probe 96-well plate. The cells were added to the top of the filter and incubated for 2 h at 37°C. After incubation, the top of the filter was washed five times with medium, and fluorescence intensity of the bottom well plate was measured in a Perkin Elmer fluorescence microplate reader. The experiment was repeated three times in triplicate. $*p < 0.05$, $**p < 0.01$, $***p < 0.001$, Student t test.

resistance to receptor phosphorylation, desensitization, and internalization (46) (Figs. 3C, 3D, 6B, 6C).

Although GRK2 and GRK6 appeared to be the important GRKs in CXCR1 and CXCR2 regulation, respectively, the possibility exists that other isoform(s) may participate in receptor-mediated postendocytic signals. Indeed, GRK2 depletion significantly attenuated CXCR1-mediated ERK1/2 activation, whereas response to CXCR2 was not affected by GRK2 or GRK6 inhibition (Fig. 5). The V2 vasopressin receptor was shown to couple to GRK2 and

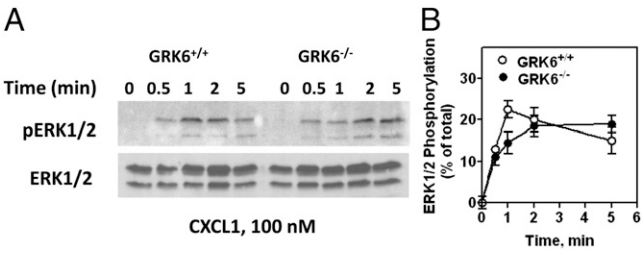

FIGURE 7. CXCL1-induced ERK activity. (**A**) Zymosan-elicited peritoneal neutrophils from $GRK6^{-/-}$ and $GRK6^{+/+}$ mice were treated with CXCL1 for different periods of time. Cell lysates were assayed for ERK phosphorylation using phospho-ERK Ab. (**B**) The extent of ERK1/2 phosphorylation is expressed as percentage of total ERK1/2 and is the average of three experiments.

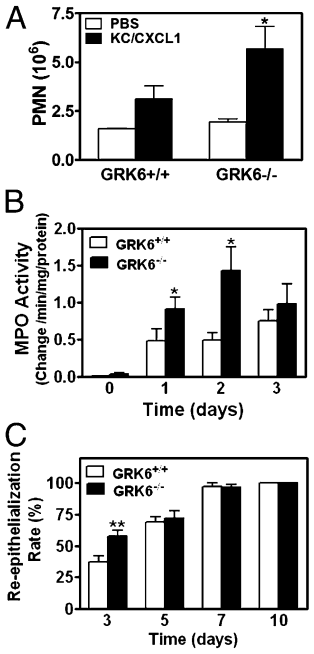

FIGURE 8. Effect of GRK6 knockdown on leukocyte migration, MPO activity, and wound re-epithelialization. (**A**) Six-day air pouches were raised in the dorsum of 6–8-wk-old $GRK6^{-/-}$ mice and their littermates ($GRK6^{+/+}$). Mice were injected with 0.5 ml PBS or PBS containing murine CXCL1 (100 pmol). Exudates were collected after 4 h, and the total number of leukocytes (~90% neutrophils) was enumerated. (**B**) Wound extracts from $GRK6^{-/-}$ and wild-type $GRK6^{+/+}$ mice were harvested, and MPO activity within each wound bed was determined spectrophotometrically. The mean ± SEM value of four wounds for each time point for each mouse genotype is shown. (**C**) Percentage of epidermal resurfacing for wounds from wild-type $GRK6^{+/+}$ and $GRK6^{-/-}$ animals was measured on days 3, 5, 7, and 10, as described in *Materials and Methods*. The value for each time point is the mean ± SEM of eight wounds. $*p < 0.05$, $**p < 0.01$, Student t test.

GRK3 to undergo receptor phosphorylation and desensitization, but it couples to GRK5 and GRK6 to mediate postendocytic signals, including ERK1/2 activation (49). C3aR desensitization and internalization are also mediated through GRK2- and GRK3-dependent pathways, whereas exocytosis and MAPK activation are modulated through GRK5 and GRK6 (46). CCR7 was also shown to couple to both GRK3 and GRK6 to undergo phosphorylation and desensitization, but only GRK6 phosphorylation led to MAPK activation (18). CXCR4 was shown to couple to GRK2, GRK3, and GRK6 to modulate ERK1/2 activation (20).

Inhibition of GRK2 in RBL-2H3 cells totally prevented CXCR1 endocytosis (~40% versus ~100% for $GRK2^{+/+}$ and $GRK2^{-/-}$ cells, respectively, after 60 min, Fig. 4E), whereas the effect of GRK6 depletion on CXCR2 was partial (~5% versus ~65% for $GRK6^{+/+}$ and $GRK6^{-/-}$ cells, respectively, after 60 min, Fig. 3C). Previous studies using transfected cells lines expressing wild-type and mutant receptors showed that, in addition to GRK-mediated receptor phosphorylation and arrestin-dependent internalization, CXCR2 internalizes through a receptor phosphorylation/arrestin-independent process (5, 32). Thus, this partial inhibition of receptor internalization may be due to the receptor's ability to scaffold to other adaptor protein, such as adaptor protein-2 and the heat shock cognate/heat shock protein 70-interacting protein, to internalize (50, 51). Supporting that contention is that, in mouse embryonic fibroblasts deficient in both β-arrestin-1 and β-arrestin-2 ($\beta arr1/2^{-/-}$), CXCR2 internalization was simply delayed relative to control mouse embryonic fibroblasts ($\beta arr1/2^{+/+}$) (48).

In summary, the data in this study indicate that GRK2 and GRK6 negatively regulate CXCR1- and CXCR2-mediated neutrophil functions. However, two questions remain to be addressed. First, under physiological conditions, CXCL8 exists as a mixture of dimer and monomer (52). It was previously shown that the monomeric and dimeric forms of CXCL8 differ in their ability to activate and regulate CXCR1 and CXCR2 (33). Thus, it is possible that the monomer/receptor and dimer/receptor complexes may couple to different GRK isoforms to mediate and regulate cellular responses. Second, using receptor-specific Abs, it was recently shown that phosphorylation of specific serine or threonine residues on the cytoplasmic tail of the β2-adrenergic receptor and CXCR4 by specific GRKs governs the ability of the receptors to complex with β-arrestins and modulate cellular activities (53). CXCR1 and CXCR2 possess several serine and threonine residues in their cytoplasmic tails, which are critical for receptor phosphorylation, desensitization, downregulation, and postendocytic activities (5). Thus, defining the specific role of these residues in receptor activation and regulation may provide new insights into the role of CXCL8 in inflammation, tumor progression, and metastasis, as well as new targets for therapeutic interventions.

Acknowledgments

We thank Dr. Robert J. Lefkowitz (Howard Hughes Medical Institute, Duke University Medical Center) for providing the GRK6-deficient mouse model. We are very thankful to Nikia Smith, Kimberly M. Malloy, and Angela Isley (Julius L. Chambers Biomedical/Biotechnology Research Institute) for technical support. We thank Kelly S. Parman (Mouse Pathology and Immunohistochemistry Core Lab, Vanderbilt University Medical Center) for technical support with mouse tissue processing and immunostaining and Yingchun Yu (Department of Cancer Biology, Vanderbilt University Medical Center) for technical assistance with the wound-healing and MPO assays.

Disclosures

The authors have no financial conflicts of interest.

References

1. Baggiolini, M. 2000. Reflections on chemokines. *Immunol. Rev.* 177: 5–7.
2. Murphy, P. M., M. Baggiolini, I. F. Charo, C. A. Hébert, R. Horuk, K. Matsushima, L. H. Miller, J. J. Oppenheim, and C. A. Power. 2000. International union of pharmacology. XXII. Nomenclature for chemokine receptors. *Pharmacol. Rev.* 52: 145–176.
3. Baggiolini, M., B. Dewald, and B. Moser. 1997. Human chemokines: an update. *Annu. Rev. Immunol.* 15: 675–705.
4. Richardson, R. M., B. C. Pridgen, B. Haribabu, H. Ali, and R. Snyderman. 1998. Differential cross-regulation of the human chemokine receptors CXCR1 and CXCR2. Evidence for time-dependent signal generation. *J. Biol. Chem.* 273: 23830–23836.
5. Richardson, R. M., R. J. Marjoram, L. S. Barak, and R. Snyderman. 2003. Role of the cytoplasmic tails of CXCR1 and CXCR2 in mediating leukocyte migration, activation, and regulation. *J. Immunol.* 170: 2904–2911.
6. Yang, W., D. Wang, and A. Richmond. 1999. Role of clathrin-mediated endocytosis in CXCR2 sequestration, resensitization, and signal transduction. *J. Biol. Chem.* 274: 11328–11333.
7. Neel, N. F., E. Schutyser, J. Sai, G. H. Fan, and A. Richmond. 2005. Chemokine receptor internalization and intracellular trafficking. *Cytokine Growth Factor Rev.* 16: 637–658.
8. Vroon, A., C. J. Heijnen, and A. Kavelaars. 2006. GRKs and arrestins: regulators of migration and inflammation. *J. Leukoc. Biol.* 80: 1214–1221.
9. Reiter, E., and R. J. Lefkowitz. 2006. GRKs and beta-arrestins: roles in receptor silencing, trafficking and signaling. *Trends Endocrinol. Metab.* 17: 159–165.
10. Pitcher, J. A., N. J. Freedman, and R. J. Lefkowitz. 1998. G protein-coupled receptor kinases. *Annu. Rev. Biochem.* 67: 653–692.
11. Premont, R. T., and R. R. Gainetdinov. 2007. Physiological roles of G protein-coupled receptor kinases and arrestins. *Annu. Rev. Physiol.* 69: 511–534.
12. Cho, D., M. Zheng, C. Min, L. Ma, H. Kurose, J. H. Park, and K. M. Kim. 2010. Agonist-induced endocytosis and receptor phosphorylation mediate resensitization of dopamine D(2) receptors. *Mol. Endocrinol.* 24: 574–586.
13. Sallese, M., L. Salvatore, E. D'Urbano, G. Sala, M. Storto, T. Launey, F. Nicoletti, T. Knöpfel, and A. De Blasi. 2000. The G-protein-coupled receptor kinase GRK4 mediates homologous desensitization of metabotropic glutamate receptor 1. *FASEB J.* 14: 2569–2580.
14. Luo, J., J. M. Busillo, and J. L. Benovic. 2008. M3 muscarinic acetylcholine receptor-mediated signaling is regulated by distinct mechanisms. *Mol. Pharmacol.* 74: 338–347.
15. de Jager, S. C., B. Bermúdez, I. Bot, R. R. Koenen, M. Bot, A. Kavelaars, V. de Waard, C. J. Heijnen, F. J. Muriana, C. Weber, et al. 2011. Growth differentiation factor 15 deficiency protects against atherosclerosis by attenuating CCR2-mediated macrophage chemotaxis. *J. Exp. Med.* 208: 217–225.
16. Vroon, A., C. J. Heijnen, M. S. Lombardi, P. M. Cobelens, F. Mayor, Jr., M. G. Caron, and A. Kavelaars. 2004. Reduced GRK2 level in T cells potentiates chemotaxis and signaling in response to CCL4. *J. Leukoc. Biol.* 75: 901–909.
17. Kleibeuker, W., M. Jurado-Pueyo, C. Murga, N. Eijkelkamp, F. Mayor, Jr., C. J. Heijnen, and A. Kavelaars. 2008. Physiological changes in GRK2 regulate CCL2-induced signaling to ERK1/2 and Akt but not to MEK1/2 and calcium. *J. Neurochem.* 104: 979–992.
18. Zidar, D. A., J. D. Violin, E. J. Whalen, and R. J. Lefkowitz. 2009. Selective engagement of G protein coupled receptor kinases (GRKs) encodes distinct functions of biased ligands. *Proc. Natl. Acad. Sci. USA* 106: 9649–9654.
19. Vroon, A., C. J. Heijnen, R. Raatgever, I. P. Touw, R. E. Ploemacher, R. T. Premont, and A. Kavelaars. 2004. GRK6 deficiency is associated with enhanced CXCR4-mediated neutrophil chemotaxis in vitro and impaired responsiveness to G-CSF in vivo. *J. Leukoc. Biol.* 75: 698–704.
20. Busillo, J. M., S. Armando, R. Sengupta, O. Meucci, M. Bouvier, and J. L. Benovic. 2010. Site-specific phosphorylation of CXCR4 is dynamically regulated by multiple kinases and results in differential modulation of CXCR4 signaling. *J. Biol. Chem.* 285: 7805–7817.
21. Prado, G. N., H. Suzuki, N. Wilkinson, B. Cousins, and J. Navarro. 1996. Role of the C terminus of the interleukin 8 receptor in signal transduction and internalization. *J. Biol. Chem.* 271: 19186–19190.
22. Ben-Baruch, A., K. M. Bengali, A. Biragyn, J. J. Johnston, J. M. Wang, J. Kim, A. Chuntharapai, D. F. Michiel, J. J. Oppenheim, and D. J. Kelvin. 1995. Interleukin-8 receptor beta. The role of the carboxyl terminus in signal transduction. *J. Biol. Chem.* 270: 9121–9128.
23. Matityahu, E., R. Feniger-Barish, T. Meshel, A. Zaslaver, and A. Ben-Baruch. 2002. Intracellular trafficking of human CXCR1 and CXCR2: regulation by receptor domains and actin-related kinases. *Eur. J. Immunol.* 32: 3525–3535.
24. Ali, H., R. M. Richardson, E. D. Tomhave, J. R. Didsbury, and R. Snyderman. 1993. Differences in phosphorylation of formylpeptide and C5a chemoattractant receptors correlate with differences in desensitization. *J. Biol. Chem.* 268: 24247–24254.
25. Nasser, M. W., S. K. Raghuwanshi, K. M. Malloy, P. Gangavarapu, J. Y. Shim, K. Rajarathnam, and R. M. Richardson. 2007. CXCR1 and CXCR2 activation and regulation. Role of aspartate 199 of the second extracellular loop of CXCR2 in CXCL8-mediated rapid receptor internalization. *J. Biol. Chem.* 282: 6906–6915.
26. Richardson, R. M., B. C. Pridgen, B. Haribabu, and R. Snyderman. 2000. Regulation of the human chemokine receptor CCR1. Cross-regulation by CXCR1 and CXCR2. *J. Biol. Chem.* 275: 9201–9208.
27. Ali, H., E. D. Tomhave, R. M. Richardson, B. Haribabu, and R. Snyderman. 1996. Thrombin primes responsiveness of selective chemoattractant receptors at a site distal to G protein activation. *J. Biol. Chem.* 271: 3200–3206.
28. Nasser, M. W., R. J. Marjoram, S. L. Brown, and R. M. Richardson. 2005. Cross-desensitization among CXCR1, CXCR2, and CCR5: role of protein kinase C-epsilon. *J. Immunol.* 174: 6927–6933.
29. Brown, S. L., V. R. Jala, S. K. Raghuwanshi, M. W. Nasser, B. Haribabu, and R. M. Richardson. 2006. Activation and regulation of platelet-activating factor receptor: role of G(i) and G(q) in receptor-mediated chemotactic, cytotoxic, and cross-regulatory signals. *J. Immunol.* 177: 3242–3249.
30. Fong, A. M., R. T. Premont, R. M. Richardson, Y. R. Yu, R. J. Lefkowitz, and D. D. Patel. 2002. Defective lymphocyte chemotaxis in beta-arrestin2- and GRK6-deficient mice. *Proc. Natl. Acad. Sci. USA* 99: 7478–7483.
31. Raghuwanshi, S. K., M. W. Nasser, X. Chen, R. M. Strieter, and R. M. Richardson. 2008. Depletion of beta-arrestin-2 promotes tumor growth and angiogenesis in a murine model of lung cancer. *J. Immunol.* 180: 5699–5706.
32. Su, Y., S. K. Raghuwanshi, Y. Yu, L. B. Nanney, R. M. Richardson, and A. Richmond. 2005. Altered CXCR2 signaling in beta-arrestin-2-deficient mouse models. *J. Immunol.* 175: 5396–5402.
33. Nasser, M. W., S. K. Raghuwanshi, D. J. Grant, V. R. Jala, K. Rajarathnam, and R. M. Richardson. 2009. Differential activation and regulation of CXCR1 and CXCR2 by CXCL8 monomer and dimer. *J. Immunol.* 183: 3425–3432.
34. Edwards, J. C., A. D. Sedgwick, and D. A. Willoughby. 1981. The formation of a structure with the features of synovial lining by subcutaneous injection of air: an in vivo tissue culture system. *J. Pathol.* 134: 147–156.
35. Sin, Y. M., A. D. Sedgwick, E. P. Chea, and D. A. Willoughby. 1986. Mast cells in newly formed lining tissue during acute inflammation: a six day air pouch model in the mouse. *Ann. Rheum. Dis.* 45: 873–877.
36. Clish, C. B., J. A. O'Brien, K. Gronert, G. L. Stahl, N. A. Petasis, and C. N. Serhan. 1999. Local and systemic delivery of a stable aspirin-triggered lipoxin prevents neutrophil recruitment in vivo. *Proc. Natl. Acad. Sci. USA* 96: 8247–8252.
37. Devalaraja, R. M., L. B. Nanney, J. Du, Q. Qian, Y. Yu, M. N. Devalaraja, and A. Richmond. 2000. Delayed wound healing in CXCR2 knockout mice. *J. Invest. Dermatol.* 115: 234–244.
38. Milatovic, S., L. B. Nanney, Y. Yu, J. R. White, and A. Richmond. 2003. Impaired healing of nitrogen mustard wounds in CXCR2 null mice. *Wound Repair Regen.* 11: 213–219.
39. Nanney, L. B. 1990. Epidermal and dermal effects of epidermal growth factor during wound repair. *J. Invest. Dermatol.* 94: 624–629.

40. Thorey, I. S., B. Hinz, A. Hoeflich, S. Kaesler, P. Bugnon, M. Elmlinger, R. Wanke, E. Wolf, and S. Werner. 2004. Transgenic mice reveal novel activities of growth hormone in wound repair, angiogenesis, and myofibroblast differentiation. *J. Biol. Chem.* 279: 26674–26684.
41. Damaj, B. B., S. R. McColl, K. Neote, C. A. Hébert, and P. H. Naccache. 1996. Diverging signal transduction pathways activated by interleukin 8 (IL-8) and related chemokines in human neutrophils. IL-8 and Gro-alpha differentially stimulate calcium influx through IL-8 receptors A and B. *J. Biol. Chem.* 271: 20540–20544.
42. Richardson, R. M., R. A. DuBose, H. Ali, E. D. Tomhave, B. Haribabu, and R. Snyderman. 1995. Regulation of human interleukin-8 receptor A: identification of a phosphorylation site involved in modulating receptor functions. *Biochemistry* 34: 14193–14201.
43. Feniger-Barish, R., M. Ran, A. Zaslaver, and A. Ben-Baruch. 1999. Differential modes of regulation of cxc chemokine-induced internalization and recycling of human CXCR1 and CXCR2. *Cytokine* 11: 996–1009.
44. Barlic, J., J. D. Andrews, A. A. Kelvin, S. E. Bosinger, M. E. DeVries, L. Xu, T. Dobransky, R. D. Feldman, S. S. Ferguson, and D. J. Kelvin. 2000. Regulation of tyrosine kinase activation and granule release through beta-arrestin by CXCRI. *Nat. Immunol.* 1: 227–233.
45. Chuntharapai, A., and K. J. Kim. 1995. Regulation of the expression of IL-8 receptor A/B by IL-8: possible functions of each receptor. *J. Immunol.* 155: 2587–2594.
46. Guo, Q., H. Subramanian, K. Gupta, and H. Ali. 2011. Regulation of C3a receptor signaling in human mast cells by G protein coupled receptor kinases. *PLoS ONE* 6: e22559.
47. Vibhuti, A., K. Gupta, H. Subramanian, Q. Guo, and H. Ali. 2011. Distinct and shared roles of β-arrestin-1 and β-arrestin-2 on the regulation of C3a receptor signaling in human mast cells. *PLoS ONE* 6: e19585.
48. Zhao, M., A. Wimmer, K. Trieu, R. G. Discipio, and I. U. Schraufstatter. 2004. Arrestin regulates MAPK activation and prevents NADPH oxidase-dependent death of cells expressing CXCR2. *J. Biol. Chem.* 279: 49259–49267.
49. Ren, X. R., E. Reiter, S. Ahn, J. Kim, W. Chen, and R. J. Lefkowitz. 2005. Different G protein-coupled receptor kinases govern G protein and beta-arrestin-mediated signaling of V2 vasopressin receptor. *Proc. Natl. Acad. Sci. USA* 102: 1448–1453.
50. Fan, G. H., W. Yang, X. J. Wang, Q. Qian, and A. Richmond. 2001. Identification of a motif in the carboxyl terminus of CXCR2 that is involved in adaptin 2 binding and receptor internalization. *Biochemistry* 40: 791–800.
51. Barker, B. L., and J. L. Benovic. 2011. G protein-coupled receptor kinase 5 phosphorylation of hip regulates internalization of the chemokine receptor CXCR4. *Biochemistry* 50: 6933–6941.
52. Burrows, S. D., M. L. Doyle, K. P. Murphy, S. G. Franklin, J. R. White, I. Brooks, D. E. McNulty, M. O. Scott, J. R. Knutson, D. Porter, et al. 1994. Determination of the monomer-dimer equilibrium of interleukin-8 reveals it is a monomer at physiological concentrations. *Biochemistry* 33: 12741–12745.
53. Tran, T. M., R. Jorgensen, and R. B. Clark. 2007. Phosphorylation of the beta2-adrenergic receptor in plasma membranes by intrinsic GRK5. *Biochemistry* 46: 14438–14449.